

## Photoalignment of Poly(di-*n*-hexylsilane) by Azobenzene Monolayer. 2. Structural Optimization of the Surface Azobenzene Monolayer

Kazuyuki Fukuda and Takahiro Seki\*

Photofunctional Chemistry Division, Chemical Resources Laboratory, Tokyo Institute of Technology, 4259 Nagatuta, Midori-ku, Yokohama, 226-8503, Japan

Kunihiro Ichimura

Research Laboratory for Science and Technology, Science University of Tokyo, 2641 Yamazaki, Noda, Chiba 278-8510, Japan

Received August 13, 2001

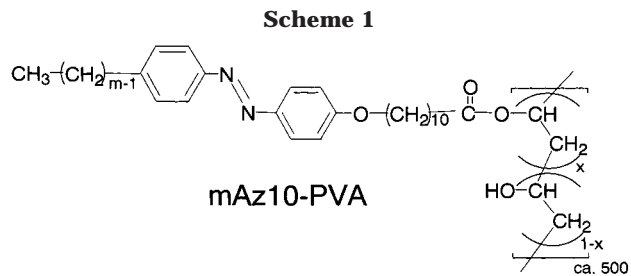
**ABSTRACT:** For the optimization of the surface-mediated photoalignment process of a poly(di-*n*-hexylsilane) (PDHS) film, a systematic investigation was conducted with respect to the design of the surface azobenzene (Az) monolayer. The preparative conditions and synthetic design of the Az monolayer were investigated in terms of exposure energy, lateral packing density, and length of *n*-alkyl tail attached to the Az units. The in-plane dichroic ratio of the Az monolayer was enhanced monotonically with increased exposure energy of the linearly polarized visible light (LPL) from 0.15 to 3.0 J cm<sup>-2</sup>. A good correlation was obtained for the orientational order of PDHS with the dichroic ratio of the Az monolayer. The lateral packing density was varied by changing the level of compression in the LB deposition process. The highest orientational order of PDHS was obtained for the Az monolayer at ca. 0.4 nm<sup>2</sup> per Az unit. The alignment behavior of PDHS was further dependent on the tail length of Az unit. The most efficient in-plane control was achieved for the Az monolayer having an octyl (C8) tail. As a whole, the Az monolayer having the octyl tail prepared at 0.4 nm<sup>2</sup> per Az after exposure to 3.0 J cm<sup>-2</sup> of LPL yielded the highest anisotropy, leading to the highest order parameter of the PDHS film reaching ca. 0.7. Micropatterned irradiation through a photomask performed in the above-optimized conditions provided a locally addressed uniaxial alignment at a resolution of 6 μm.

### 1. Introduction

Irradiation with linearly polarized light (LPL) to polymer films involving an azobenzene (Az) unit results in an molecular orientational anisotropy in the film.<sup>1,2</sup> The rod-shaped trans isomer of azobenzenes absorbs photons of LPL proportionally to cos<sup>2</sup> Θ of the energy whereas Θ is the angle between the molecular axis and the electric vector of the light.<sup>3</sup> Az units are subjected to angular-selective isomerization, followed by angular redistribution and rotational diffusion to minimize light absorption through the reversible cis/trans photoisomerization cycles.<sup>4</sup> Many examples are hitherto known for liquid crystalline (LC) materials where molecular alignment is controlled by the anisotropic excitation with LPL.<sup>3,5</sup> For low molecular mass nematic LCs, the molecular alignment is readily controlled via the orientational transfer from a photoreactive molecular or polymer layer attached on a substrate surface.<sup>2,6</sup>

Our recent work revealed that essentially the same surface transfer process is applicable for a spin-cast film of poly(di-*n*-hexylsilane) (PDHS).<sup>7,8</sup> The PDHS chain is aligned perpendicular direction to the polarization plane of the actinic LPL, namely, the direction of the long axis of Az. In the previous paper,<sup>8</sup> effects of preparative conditions affecting the orienting behavior of PDHS and resulting morphological features are described in detail. Following these results, the present paper reports on the structural optimization of the surface Az monolayer prepared by the Langmuir–Blodgett (LB) method.

Much knowledge has been accumulated on the LPL-induced molecular reorientation in photochromic LB



films (mostly Az systems).<sup>9–14</sup> However, little attention has been paid to what extents the lateral packing density and structural modification of the molecular structure affect the photoorientation behavior. Our previous approach using LB monolayers of an Az-containing poly(vinyl alcohol)s showed great influences of the lateral packing density on the alignment behavior of nematic LCs.<sup>15,16</sup> Furthermore, changes in the molecular structure at the alkylene spacer and alkyl tail attached to the Az part have been found to influence greatly to the molecular cooperativity with LCs.<sup>16–19</sup> In these contexts, the investigation on the design of the surface Az monolayer for the photoalignment of PDHS film should be of particular importance.

### 2. Experimental Section

**2.1. Materials.** The synthetic procedure of 6Az10-PVA was described previously.<sup>18,20</sup> The other series of *m*Az10-PVA (*m* = 2, 4, 7, 8, 10, and 12) (Scheme 1) were synthesized in similar manners.

Here, the synthetic procedure for *m* = 12 is only described as the typical example. The Az carboxylic acid derivatives, 11-[4-((4-dodecylphenyl)azo)phenoxy]undecanoic acid (12Az10-

\* To whom correspondence should be addressed: fax +81-45-924-5247; e-mail tseki@res.titech.ac.jp.

**Table 1. Synthesis of *m*Az10-PVA**

<i>m</i>	Az carboxylic acid derivatives (g) <sup>a</sup>	reaction time (h)	yield (%)	<i>x</i> <sup>b</sup>
2	0.822	48	70	0.11
4	0.877	83	43	0.18
6	0.933	90	42	0.23
7	0.961	94	55	0.28
8	0.989	102	53	0.20
10	1.046	120	60	0.26
12	1.102	137	76	0.23

<sup>a</sup> The amount of PVA was 0.080 g (0.0018 mol) for all batches. The molar amount of Az carboxylic acid (*m*Az10COOH) was 0.002 mol for all cases. <sup>b</sup> Resulting content of Az side chain estimated by UV-vis spectroscopy.

COOH), was prepared as mentioned in the previous paper.<sup>18,19</sup> Poly(vinyl alcohol) (0.080 g, 0.018 mol, degree of polymerization = 500, fully saponified, Nihon Gosei Chemical Industry Co.) was dissolved in dry *N,N*-dimethylacetamide (DMA, 4 mL) on heating (130 °C) and then cooled to 70 °C. 12Az10COOH (1.102 g, 0.002 mol) and 2,4,6-trinitrochlorobenzene (0.494 g, 0.006 mol, Tokyo Kasei Kogyo Co., Ltd.) dissolved in 4 mL of DMA were added to the polymer solution at 70 °C, and then a portion of dry pyridine (0.494 g, 0.006 mol) was successively added. In 24 h, the polymeric product started to precipitate partially, and 1 mL of dry benzene was then added, which allowed a clear homogeneous reaction system. The solution was further heated at 70 °C for 137 h. After cooling to room temperature, the viscous polymer solution was poured into 500 mL of methanol to obtain a precipitate of the target polymeric product. The precipitate was dissolved in chloroform again and reprecipitated by pouring into methanol/acetone (volume 1:1, 500 mL) to obtain 0.25 g (yield 76%) of the purified polymer product. Thin-layer chromatography on silica gel using ethyl acetate gave the product spot at *R<sub>f</sub>* = 0, in contrast to that of 12Az10COOH at *R<sub>f</sub>* = 0.75. The other families of *m*Az10-PVA (*m* = 2, 4, 6, 7, 8, 10) were prepared in the same manners as to the synthesis of 12Az10-PVA. The reaction rate of the condensation reaction became smaller for the Az compound with the longer tail. Therefore, the reaction time of esterification was changed accordingly. The degree of esterification was determined spectrophotometrically using the molar extinction coefficient of Az at 350 nm ( $2.9 \times 10^4$  cm<sup>2</sup> dm<sup>3</sup> mol<sup>-1</sup>). The synthetic conditions and the resulting copolymerization ratios are summarized in Table 1.

Synthetic procedures of PDHS, their characterizations, and the cleaning method of the fused silica plates were described in the previous paper.<sup>8</sup> In this work, PDHS having low molecular weight ( $M_w = 2.5 \times 10^4$ ,  $M_w/M_n = 2.7$ ) was employed. The LB monolayers of *m*Az10-PVA were prepared on a LAUDA film balance FW-II at 20 °C.<sup>8</sup> Spin-cast films of PDHS were prepared from hexane solutions.

**2.2. Measurements.** UV-vis absorption spectra were taken on a Hewlett-Packard diode array spectrometer 8452A or a JASCO model MAC-1 spectrometer that is suited for very weakly absorbing samples. For polarized spectra, a polarizer mounted in a rotating holder was placed in front of the samples.

The light irradiation was performed with a 150 W Hg-Xe lamp (San-ei UV supercure-230S) combined with optical filters for wavelength selection (Toshiba optical filters UV-35/UV-D36A for 365 nm illumination and Y-43/V-44 for 436 nm illumination). The light intensity was measured by an optical power meter (TQ8210, Advantest Co.).

The film thickness of the initial PDHS film was estimated by surface profilometry using a Dektak<sup>3</sup>ST (ULVAC/Sloan Co.) The film was scratched, and the height difference between the substrate surface and the film surface was evaluated. An average of more than three measurements was adopted for the value of film thickness.

Optical features of the aligned PDHS film were observed by a polarized optical microscope (BH-2, Olympus) combined with a high gain color camera (HCC-600, Flovel Co.).

Atomic force microscopic (AFM) images of Az monolayer were taken with a Seiko SPA300/SPI3700 system in the dynamic force mode at an ambient atmosphere.<sup>8</sup>

### 3. Results and Discussion

**3.1. Irradiation Conditions for the Anisotropy Induction.** In sections 3.1 and 3.2, experiments were made with 6Az10-PVA. The 6Az10-PVA monolayer was deposited onto a clean fused silica plate in the *cis* form by the vertical dipping method. The occupying area (*A<sub>oc</sub>*) was fixed at ca. 0.4 nm<sup>2</sup> per Az unit by controlling the surface pressure during the dipping procedure.<sup>21</sup> The deposited monolayer was stored in the dark over 4 days under a dry atmosphere, which allowed a complete thermal conversion to the *trans* form of Az.<sup>22</sup> The spectral peak of the  $\pi$ - $\pi^*$  transition of the resulting 6Az10-PVA monolayer was positioned at 330 nm, which showed a hypsochromic shift from that of a chloroform solution (352 nm). This indicates the formation of H-aggregate of the Az moieties in the monolayer.<sup>14</sup>

Direct photoirradiation with LPL at 436 nm to this monolayer was first carried out, but the photoinduced optical anisotropy was found to be small ( $A_{\perp}/A_{\parallel} = 1.27$ ). Therefore, two-step photoirradiation was employed. The 6Az10-PVA monolayer was first irradiated with nonpolarized UV (365 nm, 0.30 mJ cm<sup>-2</sup>) light to a photo-stationary state and then irradiated with LPL at 436 nm. This method was reported by Stumpe et al.<sup>14</sup> for side-chain LC Az polymers. In systems where the photoreorientation process is impeded in the Az film due to H-aggregation of *trans*-Az moieties, an efficient reorientation takes place after the UV light irradiation. UV irradiation destroys the aggregate, and an efficient photoinduced orientation becomes feasible.

Changes of the polarized absorption spectra of a 6Az10-PVA monolayer in the course of the second-step irradiation (LPL irradiation at 436 nm) are displayed in Figure 1a. Figure 1b shows the absorbance changes of  $A_{\perp}$  (open square) and  $A_{\parallel}$  (open circle) at 330 nm as a function of exposure energy. Here,  $A_{\perp}$  and  $A_{\parallel}$  represent absorbances observed with polarized probing light in perpendicular and parallel to the plane of the actinic polarized light. Figure 1c shows the dichroic ratio [DR =  $(R - 1)/(R + 1)$ , where  $R = A_{\perp}/A_{\parallel}$  at 330 nm] of the Az monolayer and  $\lambda_{\max}$  of  $A_{\perp}$  as a function of exposure energy. When the 6Az10-PVA monolayer was irradiated with visible LPL,  $A_{\perp}$  and  $A_{\parallel}$  at 330 nm both increased in a parallel fashion up to 50 mJ cm<sup>-2</sup>. The increases in  $A_{\perp}$  and  $A_{\parallel}$  indicate the proceeding of the *cis*-to-*trans* photoisomerization of Az. After this stage,  $A_{\parallel}$  gradually decreased whereas  $A_{\perp}$  continuously increased upon prolonged irradiation, resulting in the induction of in-plane dichroism. These profiles strongly imply that the photoreorientation process of Az proceeded by repeated photoisomerization with irradiation exceeding 100 mJ cm<sup>-2</sup>. The long axis of Az was oriented perpendicular to the polarization plane of the actinic light.

As the dichroism of Az monolayer increased, the peak position of  $A_{\perp}$  shifted to shorter wavelengths (Figure 1c), indicating that the reorientation of Az leads to the self-aggregation of Az moieties. The enhancement of the in-plane orientational order is associated with the formation of H-aggregation of Az, and the degree of orientation can be tailored by the exposure dose of LPL. Similar orientation-induced self-aggregation of Az has been observed for an out-of-plane photocontrol in polymeric LC film,<sup>3</sup> compression of Langmuir monolayers at air-water interface,<sup>23</sup> and transferred LB films.<sup>15</sup>

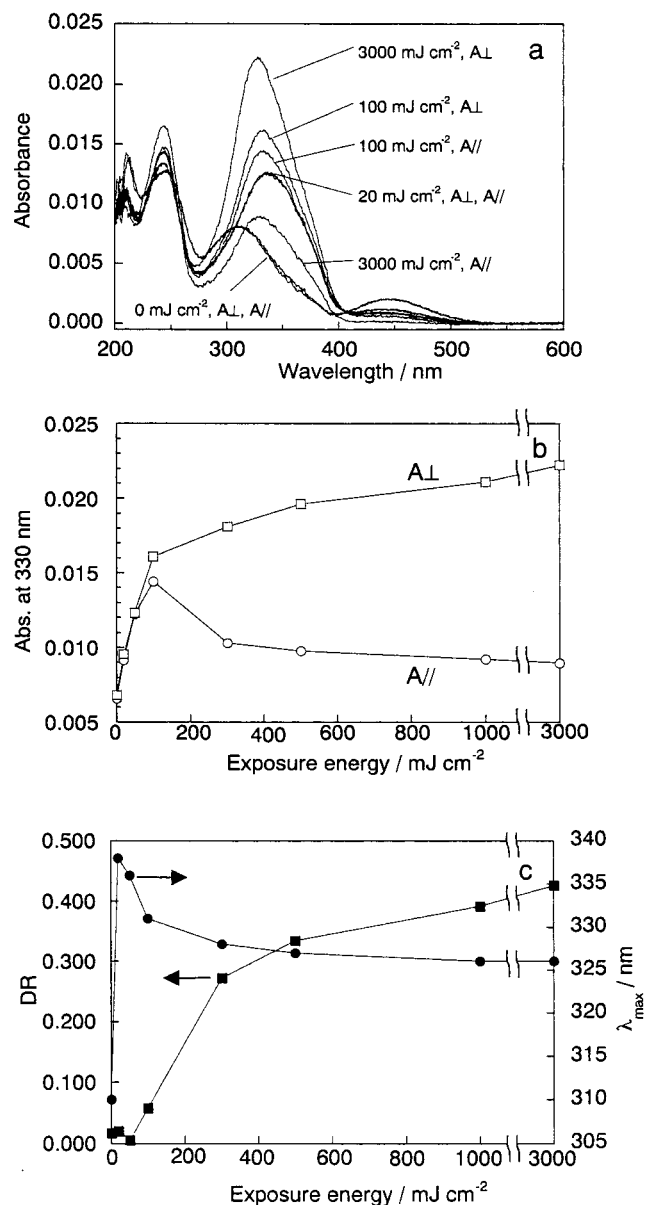


**Figure 1.** Spectroscopic data in the photoorientation of 6Az10-PVA monolayer. Changes in the polarized absorption spectra of 6Az10-PVA monolayer during the irradiation with LPL at 436 nm starting from the cis-Az state (a). Changes in absorbances [ $A_{\perp}$  (open square);  $A_{\parallel}$  (open circle)] of the 6Az10-PVA monolayer at 330 nm as a function of exposure energy (b). Changes in the dichroic ratio (DR) (closed square) and the maximum wavelength (closed circle) of  $A_{\perp}$  as a function of exposure energy (c).

Following the above knowledge, the relation between the DR of Az monolayer and the orienting behavior of PDHS film was examined. Six samples of 6Az10-PVA monolayers having different degree of DR were prepared by changing the exposure energy, and then a PDHS film (thickness = 25 nm) was prepared on these 6Az10-PVA monolayers. Immediately after spin-casting, the PDHS films were fully in a disordered phase and had no optical anisotropy. After storage of PDHS in the dark at room temperature for 2 days, the crystallized PDHS film exhibited an in-plane anisotropy.<sup>8</sup> The Si main chain of PDHS was aligned perpendicular to the polarization plane of the actinic light. Here, the orientational order of PDHS [ $S = (R - 1)/(R + 2)$ , where  $R = A_{\perp}/A_{\parallel}$ ] was strongly dependent on the exposed light dose. Figure 2 shows the DR of Az monolayer and  $S$  of PDHS as a

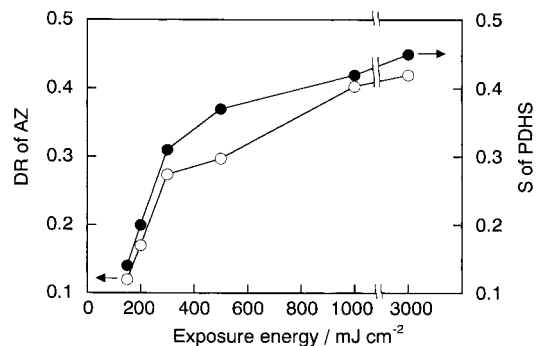


**Figure 2.** Dichroic ratio (DR) of Az monolayer (open circles) and order parameter ( $S$ ) of PDHS film (closed) as a function of exposure energy.

function of exposure energy. As clearly shown, the orientational order of the PDHS film increased almost in proportion to the increase of DR of the Az layer. In other words, the orientational order is artificially tailored by the irradiation process. This fact shows a marked contrast with the behavior of fluid nematic LCs. The order parameter of nematic LCs is in most cases governed by the intrinsic molecular assembling order of the bulk LC and insensitive to DR of the surface layer.<sup>18,24</sup> This discrepancy can be attributed to the following facts. In the PDHS films the directional correlation reaches only to local levels characterized by the sheaflike bundle structures (see Figure 6 in ref 8). For fluid LC systems, on the other hand, the monodomain is formed throughout the cell.

**3.2. Effect of Lateral Packing Density. 3.2.1. Preparative Methods for Packing Density Controls.** The lateral packing density of an LB monolayer can be readily changed by the position of the moving barrier on the water surface. This method has been actually applied for the 6Az10-PVA monolayer for elucidation of the effect of the packing density on the photoalignment behavior of nematic LCs.<sup>15,16</sup> The molecular occupying area ( $A_{oc}$ ) can be varied by changing the surface pressure for transfer. The same procedure was also carried out in the present work (method A). An alternative way to control  $A_{oc}$  is to vary the mixing ratios of the trans/cis isomers of Az in the spreading solution. Since the cis Az monolayer occupies much larger areas than the trans one at low pressures, deposition of mixed monolayers at a fixed low surface pressure (5 mN m<sup>-1</sup> in the present work) can provide a desired  $A_{oc}$  (method B).

Surface pressure–area ( $\pi$ – $A$ ) isotherms are indicated in Figure 3. The circles in the figures show the dipping points in the methods A (a) and B (b). Figure 3a shows the  $\pi$ – $A$  isotherms of cis-rich (cis content of ca. 90%) and trans-rich (cis content of ca. 20%) 6Az10-PVA monolayer applied for method A. The cis-rich and trans-rich states were obtained by irradiation with 365 and 436 nm at each photostationary state.  $A_{oc}$  was changed in the range of 0.3–1.2 nm<sup>2</sup> per Az unit by changing the surface pressure. The most dense layer (0.3 nm<sup>2</sup> per Az unit) was prepared from the trans-rich monolayer. In the plateau region of the cis-Az monolayer (0.5–0.9 nm<sup>2</sup> per Az unit), the deposition was not properly performed since the constant pressure gave rise to a large area reduction. For method B, mixed solutions were prepared with a cis-rich and a 100% trans-Az polymer solutions, and the Az monolayers were spread at given ratios (Figure 3b). The advantage of this



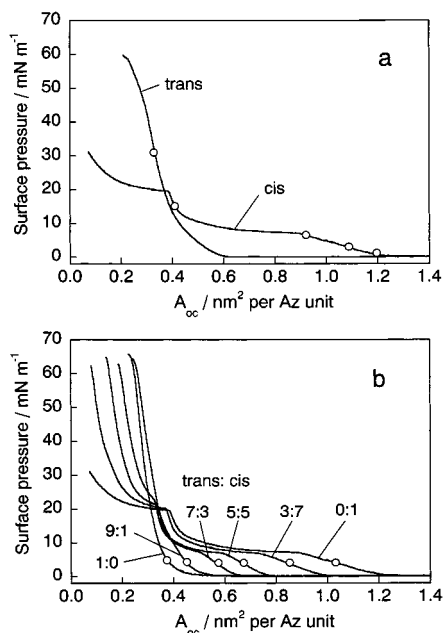


**Figure 3.** Surface pressure–area isotherms of cis-rich (cis content of ca. 90%) and trans-rich (cis content of ca. 20%) 6Az10-PVA monolayer applied for method A (a) and those of mixed 6Az10-PVA monolayer at given trans/cis molar ratios applied for method B (b). The circles show the dipping points.

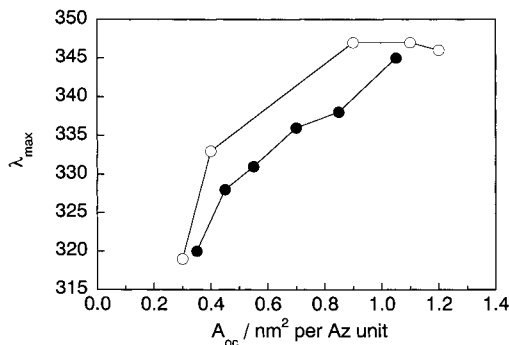


**Figure 4.** Maximum wavelength ( $\lambda_{max}$ ) of Az monolayers prepared by method A (open circles) and method B (closed) as a function of  $A_{oc}$ .

method is that the supplementary region of  $A_{oc}$  that cannot be obtained in method A (0.5–0.9 nm<sup>2</sup> per Az unit) is available.

Figure 4 depicts  $\lambda_{max}$  of the  $\pi$ – $\pi^*$  band vs  $A_{oc}$  obtained in method A (open) and B (closed). With the decrease of  $A_{oc}$ ,  $\lambda_{max}$  showed hypsochromic shifts, which became more pronounced at closely packed areas below  $A_{oc} = 0.45$  nm<sup>2</sup> per Az unit. The  $\lambda_{max}$  showed further blue shifts for monolayers obtained in method B than those in method A. This should indicate a difference in the packing homogeneity at microscopic level. In fact, AFM observations showed that the monolayers prepared by method A provided a homogeneous morphology whereas those obtained in method B showed microphase-separated structures consisting of trans Az (higher) and cis-rich Az (lower) regions. The height difference was ca. 1.5 nm (data not shown here). In the latter heterogeneous films (method B), the densely packed parts of the trans-Az film should contain further H-aggregated species, which then result in larger hypsochromic shifts on average.

**3.2.2. Photoorientation of Az Monolayer.** The prepared 6Az10-PVA LB films were irradiated with

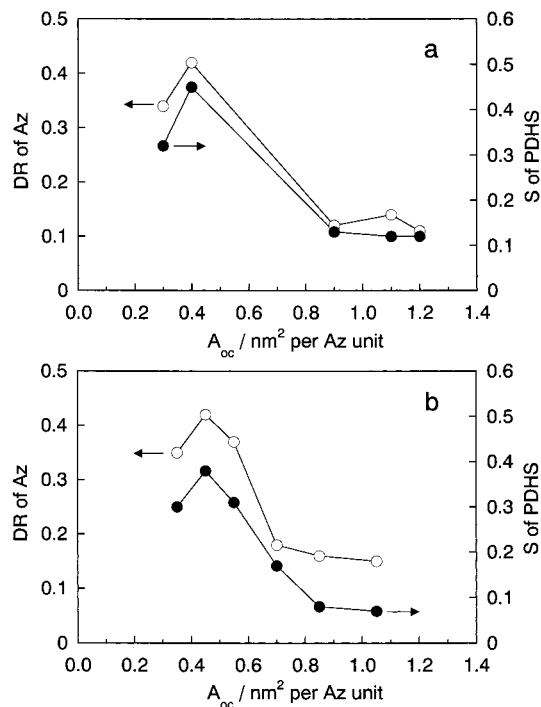


**Figure 5.** DR of Az monolayers (open) and  $S$  of PDHS films (closed) as a function of  $A_{oc}$ . The Az monolayers were prepared in method A (a) and method B (b).

nonpolarized UV (0.30 J cm<sup>-2</sup>) and then LPL at 436 nm (3.0 J cm<sup>-2</sup>). Figure 5 (open circles) shows the resulting DR of the Az monolayer prepared in method A (a) and method B (b).

At  $A_{oc} = 0.9$ – $1.2$  nm<sup>2</sup> per Az unit, the conversion to the cis form ( $C_{cis}$ ) at the photostationary state ranged from 80 to 90% after 365 nm illumination as estimated from the absorbance change at 350 nm.<sup>20</sup> Thus, the cis-to-trans photoisomerization efficiently proceeded. However, the reorientation after subsequent illumination of LPL at 436 nm was insufficient, yielding DR below 0.2. Under these conditions, the H-aggregate was not formed (see Figure 4). It is thus concluded that, at large areas above 0.9 nm<sup>2</sup> per Az unit, Az side chains are too much sparsely dispersed in the two dimensions that photoorientation of Az layer becomes disfavored due to lack of molecular cooperativity among the Az side chains.

$C_{cis}$  at  $A_{oc}$  around 0.4 nm<sup>2</sup> per Az unit also reached to the level of 80–90% despite the fact that some H-aggregate was formed ( $\lambda_{max} =$  ca. 330 nm). At this packing density, the cooperative molecular motions were attained most efficiently without loss of motional freedom. In this condition, the strongest in-plane anisotropy was induced, giving DR = 0.42. This tendency was commonly observed for both systems of methods A and B.

At the most densely packed condition at  $A_{oc} = 0.3$  nm<sup>2</sup> per Az unit, the trans-to-cis photoisomerization was considerably suppressed ( $C_{cis} =$  ca. 50%). This should be attributed to the formation of H-aggregate at a high degree as shown from the large shift of  $\lambda_{max}$  (around 320 nm, see Figure 4). DR (=0.35) was adequately high but showed a small decrease compared to that at  $A_{oc} = 0.4$  nm<sup>2</sup> per Az unit, probably due to a depressed motional freedom for rotational diffusion of photoorientation.

**3.2.3. Alignment Behavior of PDHS.** The data of orientational order parameter ( $S$ ) of the PDHS film on the photooriented Az monolayer are shown in Figure 5

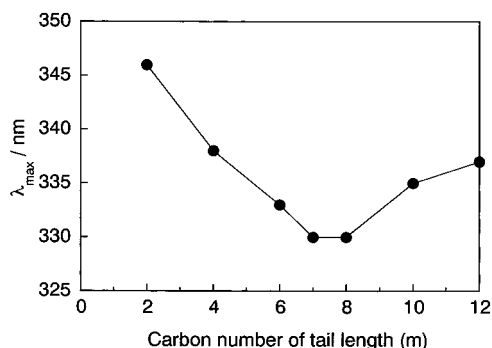


**Figure 6.** Maximum wavelength ( $\lambda_{\max}$ ) as a function of tail length ( $m$ ) in the *mAz10*-PVA monolayer. All monolayers were deposited at  $A_{oc} = 0.4 \text{ nm}^2 \text{ Az}^{-1}$ .

together with the DR data of the Az monolayer. In both series of methods A and B, a good correlation was obtained between the profiles of DR for the Az monolayer and  $S$  for the crystallized PDHS film (thickness = 25 nm). All profiles indicated a maximum at ca.  $0.4 \text{ nm}^2$  per Az unit. Thus, this is the optimum packing condition for the photoorientation of both the Az layer and PDHS film. However, slight deviations were obviously admitted between the two series of data in Figure 5a,b. DR of the Az layer was essentially the same for methods A and B, but  $S$  of the PDHS observed for method B became systematically smaller than that for method A. In other words, the orienting power of the Az monolayer prepared in method B is smaller. This may be related to the lateral microphase separation observed in Az layers obtained in method B. It seems that the phase-separated trans-Az monolayer has less orienting power since the geometrical interaction (interpenetration) between the surface layer and PDHS and also the rotational diffusion required for photoorientation should be less favored in such closely packed trans-Az layer.

**3.3. Effects of Tail Length.** The length of tail part is anticipated to influence the order of photoinduced anisotropy because the length of the alkyl chain greatly affects the molecular packing.<sup>25</sup> In the present system, the Az monolayer is anchored to the hydrophilic substrate surface via the polar PVA backbone, and the tail part is positioned to the outermost surface. PDHS should interact directly with the tail part of the Az side chain. In this context, an exploration on the tail effect is of great interest.

All the Az monolayers were prepared at a common area of ca.  $0.4 \text{ nm}^2$  per Az unit and then irradiated with UV and visible LPL. Figure 6 shows the absorption maximum ( $\lambda_{\max}$ ) of the  $\pi$ - $\pi^*$  transition as a function of carbon number of the tail. The H-aggregation, i.e., hypsochromic shift of  $\lambda_{\max}$ , was most promoted at C7 and C8. The hypsochromic shift with the increase in the tail length from C2 to C8 can be explained that the longer alkyl tail brings forth the stronger Az aggregation due to a more effective van der Waals contact. The reverse tendency (reductions of the hypsochromic shift) observed for the C10 and C12 tail may be resulted from an insufficient Az aggregation, which would be brought about by highly suppressed molecular mobility due to strong van der Waals dispersion force among the tail parts.

DR of the Az layer after photoorientation (436 nm LPL,  $3.0 \text{ J cm}^{-2}$ ) and the resulting  $S$  of PDHS (thickness = 25 nm) as a function of the carbon number of the tail

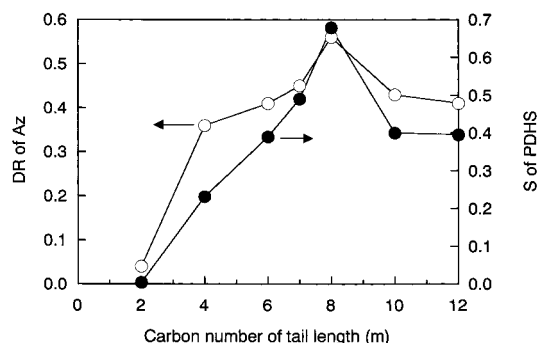


**Figure 7.** DR of Az monolayers (open) and  $S$  of PDHS films (closed) as a function of tail length ( $m$ ) in the *mAz10*-PVA monolayer.

part are shown in Figure 7. In all cases, the PDHS backbone was commonly aligned parallel to the direction of the Az monolayers, namely perpendicular to the polarization direction of the actinic light. As obviously shown, the photoinduced anisotropy of Az monolayers and  $S$  of PDHS gave the largest value in the Az monolayer having the C8 tail. DR and  $S$  were 0.56 and 0.68, respectively, for the C8 tail. Again, the magnitude of the DR had a good relationship with the degree of spectral shift in Figure 6. The monolayer showing the larger hypsochromic shift of  $\lambda_{\max}$  provided the larger DR. Thus, the higher orientational order was obtained for the monolayer containing more amounts of H-aggregated Az in the density condition of  $0.4 \text{ nm}^2$  per Az unit.

We first anticipated the length matching or recognition is important for the orientational transfer from the Az monolayer to the polymer for the combination of the C6 tail of Az and hexyl substituent of PDHS. If a series of Az monolayers having the same orientational order of Az at the identical lateral density could be prepared, one may adequately discuss the effect of the length matching. However, the present system is not the case. Preparation of such ideal series of monolayers was difficult. An Az monolayer having an odd numbered tail of (C7) was also employed. The orientation effect was to the intermediate extent of that for the C6 and C8 monolayers. Thus, the influence of the odd/even carbon number, which is observed in the alignment behavior of nematic liquid crystals on self-assembled monolayers on gold,<sup>26</sup> was not observed here. Some influences of the Az content ( $x$ ) in the copolymers (copolymerization ratio) may be included because it deviates among the polymers from 0.11 to 0.28 (see Table 1). At least apart from the C2 polymer ( $x = 0.11$ ), the deviation in  $x$  (0.18–0.28) seems of minor importance. The systematic changes in the profiles shown in Figures 5 and 6 despite the scattered values of  $x$  rationalize this assumption.

**3.4. Features of the Photoorientation of PDHS Film.** Many examples are known for epitaxial crystallization of polymers. The surfaces hitherto investigated are "rigid or fixed" surfaces such as inorganic crystals and mechanically oriented (rubbed, stretched, friction deposited) high- $T_g$  polymer surfaces. In contrast, the present work deals with "soft and flexible" molecular brush surfaces. We assume that this situation can be categorized to a new type of surfaces for epitaxial crystallization of polymers, and an emphasis can be laid on this point. The flexibility is, of course, the requirement for the achievement of photoorientation (rotational reorientation). Besides, this type of polymeric Az monolayer readily allows many variations and modifications

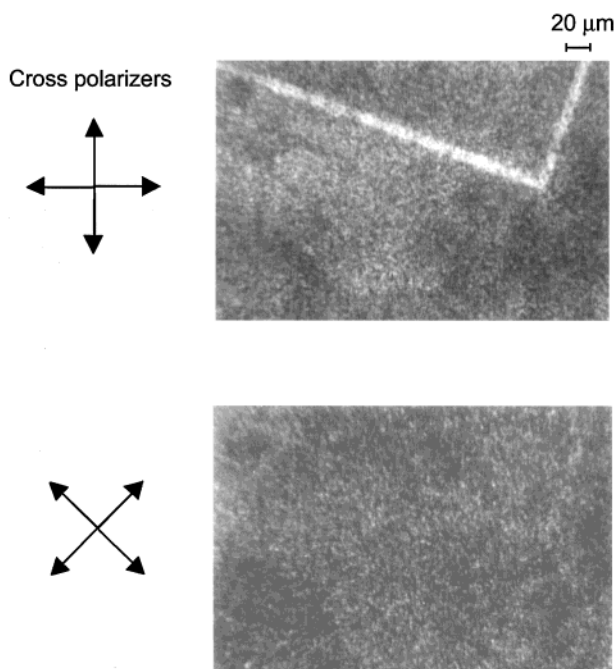


**Figure 8.** Polarized optical microscopic images of a microscopically photoaligned PDHS film (thickness = 25 nm) via LPL irradiation through a photomask. The width of bright line is ca. 6  $\mu\text{m}$ .

for the layer design. In fact, as proposed in this work, the nature of the molecular layer can be tailored by a couple of factors such as irradiation procedure, deposition condition, and molecular modification. This work reveals that a subtle change in the Az layer structure significantly influences the photoalignment behavior of PDHS. On a rigid and solid surface, the orientation and packing states of the polymer are determined by lattice matching and/or spatial requirement, and continuous and tuned modifications of the orientation in polymer films are very difficult.

A great benefit to apply the photoprocess is the feasibility of micropatterning. Figure 8 shows a polarized optical microscopic image of a locally photoaligned PDHS film as a bent line. In this experiment, the optimized conditions of photoalignment was employed: The Az layer with the C8 tail deposited at  $A_{\text{oc}} = 0.4 \text{ nm}^2$  per Az unit was irradiated with  $3.0 \text{ J cm}^{-2}$  of LPL at 436 nm. The irradiation to the Az monolayer was first performed in the above conditions through a photomask placed in contact with the surface. Onto this Az layer, the PDHS film (thickness = 25 nm) was prepared by spin-casting. The rotation of the crossed polarizers at  $45^\circ$  indicates the clear switching of emergence of disappearance of the line. This fact indicates that the bright line area is birefringent, and the PDHS chains are uniaxially aligned. The dark parts did not change its low transmission by the rotation, indicative of the random orientation of the polymer at micrometer levels. Thus, micropatterning of polymer alignment could be successfully achieved. For this example, the width of the bright line in the polarized optical microscopic image was ca. 6  $\mu\text{m}$ , which is in exact coincidence with the mask pattern (6  $\mu\text{m}$ ). In the preliminary work, we showed resolutions at the level of a hundred micrometers.<sup>7</sup> The great improvement obtained here is the consequence of the structural optimization of the Az monolayer. In the photoprocess, basically any patterned shape is applicable. It would be impossible or laborious

to attain such locally addressed orientation via mechanical or flow processes.

#### 4. Conclusions

In this work, efforts were made to optimize the design of Az monolayers for the photocontrol of PDHS chain alignment. As a general rule, the orientational order of PDHS can be directly related to the magnitude of photoinduced dichroic ratio of the underlying Az monolayer. Thus, the optimization of can be restated as the design to enlarge the in-plane anisotropy of the Az layer. Consequently, the largest orientational order of PDHS is obtained on the Az monolayer having a C8 tail at a lateral packing density of  $0.4 \text{ nm}^2$  per Az unit. It is assumed that the realization of large dichroic ratios requires the molecular cooperativity among the Az chains without loss of motional freedom for rotational diffusion. The parameters of the lateral packing density and tail length are complementary in that the former controls the in-plane ( $x$ ,  $y$ -direction) packing and the latter is related to the out-of-plane ( $z$ -direction) restriction. In both cases there is an optimum point within the conditions varied. In the optimum conditions, micropatterned alignment is feasible at a resolution of several micrometers, which shows a marked benefit compared to the conventional mechanical or flow processes. The knowledge obtained in the present work should be of great help in the extension to other types of polymers and mesostructured materials.

**Acknowledgment.** We thank Drs. S. Morino, M. Nakagawa, K. Arimitsu, and T. Ubukata for their helpful discussions. This work was financially supported by the Grand-in-Aid for Scientific Research on Priority Areas, "Molecular Synchronization for Design of New Materials System", and the Grand-in-Aid for Scientific Research (13875188 to T.S.) from the Ministry of Education, Science, Sports and Culture, Japan, and NISSAN Science Foundation.

#### References and Notes

- (1) Todorov, T.; Nikolova, L.; Tomova, N. *Appl. Opt.* **1984**, *23*, 4309.
- (2) (a) Ichimura, K. *Chem. Rev.* **2000**, *100*, 1847. (b) O'Neill, M. O.; Kelly, S. M. *J. Phys. D: Appl. Phys.* **2000**, *33*, R67.
- (3) Han, M.; Morino, S.; Ichimura, K. *Macromolecules* **2000**, *33*, 6360.
- (4) Sekkat, Z.; Dumont, M. *Proc. SPIE* **1992**, *1774*, 188.
- (5) Pedersen, T. G.; Johansen, P. M. *Phys. Rev. Lett.* **1997**, *79*, 2470.
- (6) (a) Shannon, P. J.; Gibbons, W. M.; Sun, S. T. *Nature (London)* **1994**, *368*, 532. (b) Kawanishi, Y.; Tamaki, T.; Sakuragi, M.; Seki, T.; Suzuki, Y.; Ichimura, K. *Langmuir* **1992**, *8*, 2601.
- (7) Seki, T.; Fukuda, K.; Ichimura, K. *Langmuir* **1999**, *15*, 5098.
- (8) Fukuda, K.; Seki, T.; Ichimura, K. Submitted to *Macromolecules* as part 1 of this series.
- (9) Barnik, M.; Kozenkov, V. M.; Shtykov, N. M.; Palto, S. P.; Yudin, S. G. *J. Mol. Electron.* **1989**, *5*, 53.
- (10) Unuma, Y.; Miyata, A. *Thin Solid Films* **1989**, *179*, 497.
- (11) Yokoyama, S.; Kakimoto, M.; Imai, Y. *Langmuir* **1994**, *10*, 4594.
- (12) Schönhoff, M.; Chi, L. F.; Fuchs, H.; Lösche, M. *Langmuir* **1995**, *11*, 163.
- (13) Wang, R.; Jiang, L.; Iyoda, T.; Tryk, D. A.; Hashimoto, K.; Fujishima, A. *Langmuir* **1996**, *12*, 2052.
- (14) (a) Stumpe, J.; Fischer, Th.; Menzel, H. *Macromolecules* **1996**, *29*, 2831. (b) Stumpe, J.; Geue, Th.; Fischer, Th.; Menzel, H. *Thin Solid Films* **1996**, *284*, 606. (c) Geue, Th.; Ziegler, A.; Stumpe, J. *Macromolecules* **1997**, *30*, 5729.

- (15) Seki, T.; Fukuda, R.; Tamaki, T.; Ichimura, K. *Thin Solid Films* **1994**, 243, 675.
- (16) Seki, T. *Supramol. Sci.* **1996**, 3, 25.
- (17) Seki, T.; Tamaki, T.; Suzuki, Y.; Kawanishi, Y.; Ichimura, K.; Aoki, K. *Macromolecules* **1989**, 22, 3505.
- (18) Seki, T.; Sakuragi, M.; Kawanishi, Y.; Suzuki, Y.; Tamaki, T.; Fukuda, R.; Ichimura, K. *Langmuir* **1993**, 9, 211.
- (19) Seki, T.; Ichimura, K.; Fukuda, R.; Tamaki, Y. *Kobunshi Ronbunshu* **1995**, 52, 599.
- (20) Seki, T.; Ichimura, K. *Thin Solid Films* **1989**, 179, 77.
- (21) Seki, T.; Ichimura, K. *Polym. Commun.* **1989**, 30, 108.
- (22) Seki, T.; Kojima, J.; Ichimura, K. *J. Phys. Chem. B* **1999**, 103, 10338. Seki, T.; Kojima, J.; Ichimura, K. *Macromolecules* **2000**, 33, 2709.
- (23) Kimizuka, N.; Kunitake, T. *Chem. Lett.* **1988**, 827.
- (24) Ichimura, K. *ACS Symp. Ser.* **1994**, 579, 365.
- (25) Gaines, L., Jr. In *Soluble Monolayers at Liquid-Gas Interface*; Interscience: New York, 1966.
- (26) Gupta, V. K.; Abbott, N. L. *Phys. Rev. E* **1996**, 54, R4540.

MA011459W